International Journal of Heat and Mass Transfer 71 (2014) 691–705

Contents lists available at ScienceDirect

International Journal of Heat and Mass Transfer

journal homepage: www.elsevier.com/locate/ijhmt

Effect of static contact angle on the droplet dynamics during the evaporation of a water droplet on the hot walls

Deendarlianto [a,b,*], Yasuyuki Takata [c], Sumitomo Hidaka [c], Indarto [a,b], Adhika Widyaparaga [a,b], Samsul Kamal [a,b], Purnomo [a,b], Masamichi Kohno [c]

[a] Department of Mechanical & Industrial Engineering, Faculty of Engineering, Gadjah Mada University, Jalan Grafika No. 2, Yogyakarta 55281, Indonesia
[b] Centre for Energy Studies, Gadjah Mada University, Sekip K-1A Kampus UGM, Yogyakarta 55281, Indonesia
[c] International Institute for Carbon-Neutral Energy Research (WPI-I2CNER), Department of Mechanical Engineering, Kyushu University, 744 Motooka, Nishi-ku, Fukuoka 819-0395, Japan

ARTICLE INFO

Article history:
Received 27 September 2013
Received in revised form 7 December 2013
Accepted 26 December 2013

Keywords:
Wettability
Spray cooling
Wetting limit temperature
Ultraviolet irradiation
Droplet

ABSTRACT

The effect of surface wettability on the collision dynamics and heat transfer phenomena of a single water droplet impacting upon a heated solid surface has been studied experimentally. To modify the surface wettability, two modules of stainless steel coated by TiO_2 were employed. The first module was induced by ultraviolet irradiation to produce the hydrophilic surface, while the second one was not. The diameter and the depth of coating surface were 30 mm and 200 nm, respectively. The droplet size was varied from 1.90 to 2.90 mm and substrate temperature raised up to 340 °C. The interaction of an impact water droplet with a heated solid surface was investigated using a high-speed video camera.

As a result, it was found that; (1) in the lower surface temperature region the evaporation time decreases as the static contact angle decreases, (2) the wetting limit temperature decreases with the increase of static contact angle, (3) the ultraviolet irradiation on the TiO_2 surface does not change the qualitative behavior of the evolution of wetting diameters, and (4) the maximum wetting diameter increases with the decrease of static contact angle below the wetting limit temperatures.

1. Introduction

Spray cooling is the most popular technique of water-cooling in the iron and steel making industries. It is commonly applied in the manufacture of steel, internal combustion engines, and turbine blades, in order to cool down the hot surfaces, in both very high and medium temperature regions. Spraying a hot surface with liquid droplets yields much higher heat fluxes than can be obtained by forced convective cooling. The high heat transfer rate is beneficial because they allow the size, cost, and complexity of heat exchanger equipment to be reduced. Application of spray cooling thus promotes the ability to greatly reduce production cost and develop accurate and efficient heat transfer process for the making of high quality metal product which will ultimately determine the profitability of the final product.

Understanding the physics of the phenomena is essential in order to build a model capable of predicting the heat transfer with a high accuracy. However, under practical conditions, the dispersion of the liquid results in the generation of numerous droplets which collectively can be difficult to study systematically. To investigate the underlying phenomena of spray cooling transient heat transfer characteristics in a more manageable fashion, droplet studies can be applied. The physics of a single droplet impact on heated walls can be used to predict the global heat, transfer characteristics of an entire spray [1].

Laboratory studies of spray cooling have typically measured the temperature variation and the effect of liquid properties on the evaporation [2–6]. They observed that the droplet impact dynamics depend on both substrate temperature and impact velocity. If the surface temperature is above the boiling point of the liquid, nucleate boiling will commence with vapor bubbles forming in surface crevices, detaching and rising into the liquid. Once the surface temperature rises above the "Leidenfrost point" droplets go into a state of film boiling and are seen to levitate above the solid surface, supported on a film of their own vapor. Furthermore, Moita and Moreira [7] noted also that those experiments intend to identify the fluid-dynamic regimes of the droplet interaction and to quantify the outcome of droplet impact (size, velocity and angle of ejection of secondary droplets, as well as mass deposited onto the surface).

Despite many such investigations in the past, many fundamental questions remain to be answered. One issue which has received

* Corresponding author at: Department of Mechanical & Industrial Engineering, Faculty of Engineering, Gadjah Mada University, Jalan Grafika No. 2, Yogyakarta 55281, Indonesia. Tel.: +62 274 521673.
E-mail address: deendarlianto@ugm.ac.id (Deendarliant).

0017-9310/$ - see front matter © 2014 Elsevier Ltd. All rights reserved.
http://dx.doi.org/10.1016/j.ijheatmasstransfer.2013.12.066

Nomenclature

d_o	initial droplet diameter (mm)
D	wetting diameter (mm)
D_{max}	maximum wetting diameter (mm)
Re	Reynolds number (–)
R_o	initial wetting radius (mm)
R_{max}	maximum wetting radius (mm)
T_s	surface temperature (°C)
We	Weber number (–)
Greek symbols	
β	spreading ratio, (D/d_o), (–)
σ	surface tension (N/m)
θ	contact angle (°)
μ	Viscosity (Pa s)

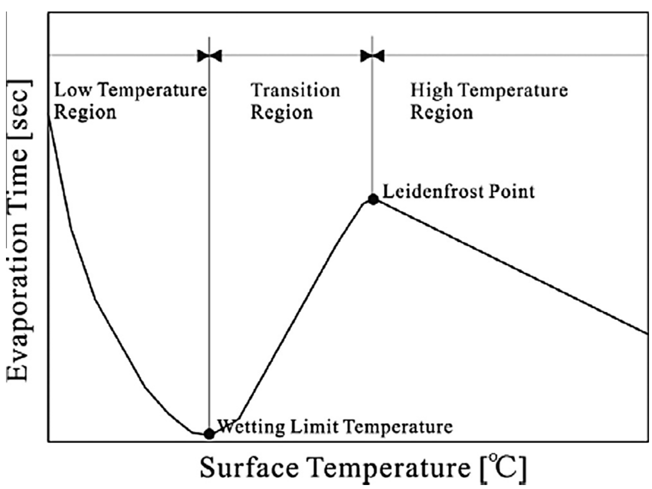

Fig. 1. Evaporation curve [13].

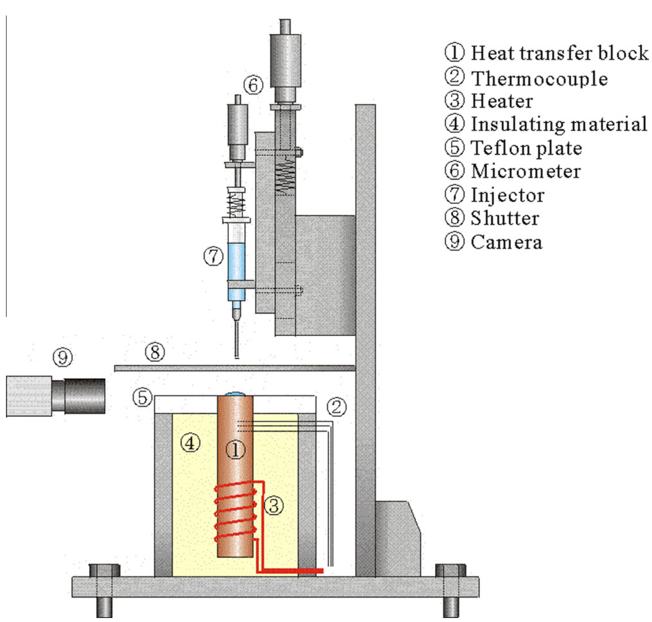

Fig. 2. Schematic diagram of the experimental apparatus.

inadequate attention is the effect of wetting angle on the evaporation of water droplet on a heated solid surface. This may be due to the difficulties of altering the static contact angle as the only exclusive parameter with all the other parameters being unchanged. The introduction of ultraviolet irradiation (UV) on the TiO_2 coating of a solid surface to alter static contact angle can be one of the solutions for this problem as reported by [8]. From this fact, we expect that heat transfer characteristics of liquid–vapor phase change phenomena like boiling and condensation can be controlled and/or enhanced by UV irradiation making use of TiO_2-coated surface. In addition, it is also important to investigate the different characteristics between TiO_2-coated surfaces and normal uncoated surfaces.

The objective of this study was to experimentally investigate the isolated effect of the static contact angle on the collision dynamics and heat transfer phenomena of a water droplet impacting upon a heated solid surface. To realize this aim, we made coated stainless steel surfaces with TiO_2. By irradiating the TiO_2 surface using UV light, the static contact angle of a droplet on

Table 1
Specification of the heat transfer surfaces.

No.	Surface treatment	Static contact angle (θ)
1	TiO_2 coating with ultraviolet irradiation (**UVW**)	0°
2	TiO_2 coating without ultraviolet irradiation (**UVN**)	(22–23)°
3	Normal stainless steel (**NS**)	88°

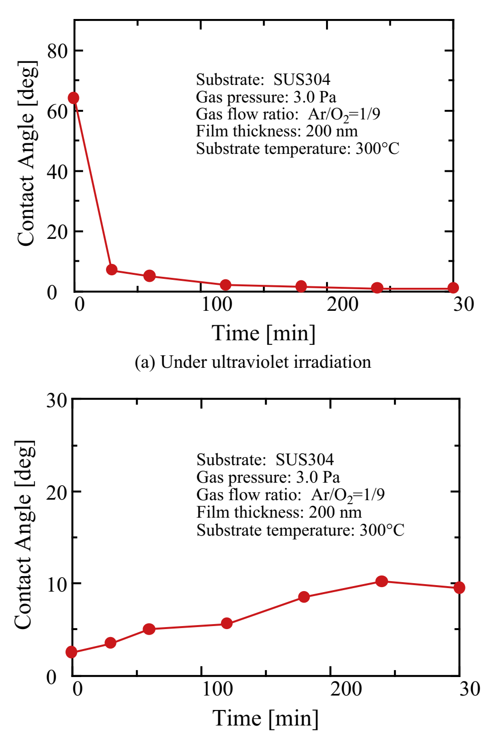

Fig. 3. Time variation of contact angle.

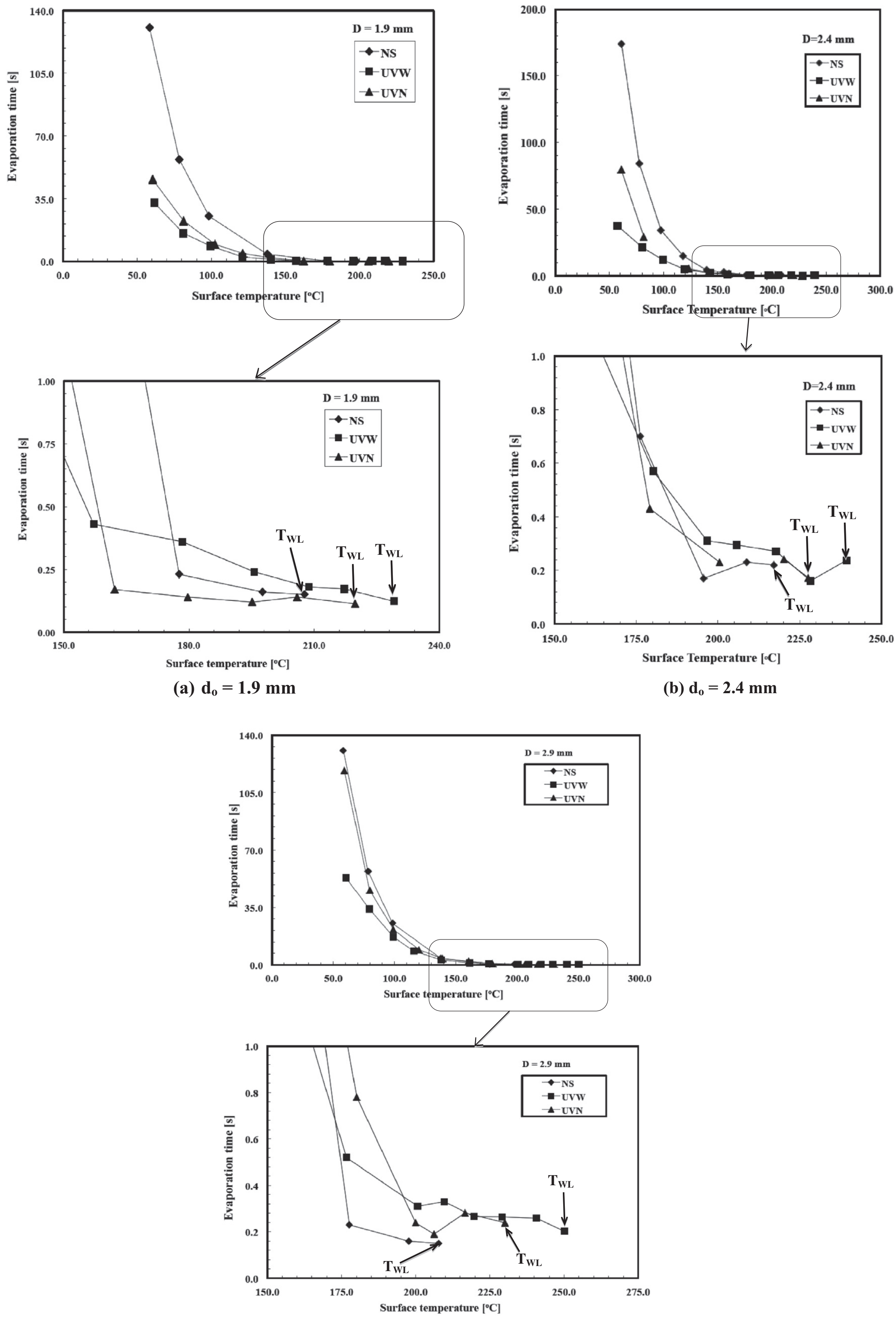

Fig. 4. Evaporation time for each tested surfaces.

the surface can be altered without disturbing other parameters such as temperature and roughness.

Table 2
Summarized of the investigated wetting limit temperature.

Surface treatment	Contact angle [°]	Wetting limit temperature [°C]		
		d_o = 1.9 mm	d_o = 2.4 mm	d_o = 2.9 mm
NS	88°	207.65	217.15	227.65
UVN	(22–23)°	219.76	227.65	230.15
UVW	0°	229.08	239.38	250.15

In the present paper, the experimental results of the photocatalytic characteristics of TiO_2 will be presented first. These data will be explained in terms of time variation of contact angle due the UV irradiation. Afterwards, the effects of surface treatments and the droplet diameters on the evaporation time will be discussed followed by the interfacial behaviors of the examined surface treatments by means of the visual observation. Finally, the effect of surface treatments, the droplet diameters, and surface temperatures on the wetted diameter for all boiling regimes will be evaluated. The maximum wetted diameter as a function of the above parameters as revealed by the data will be discussed with reference to studies by other investigators.

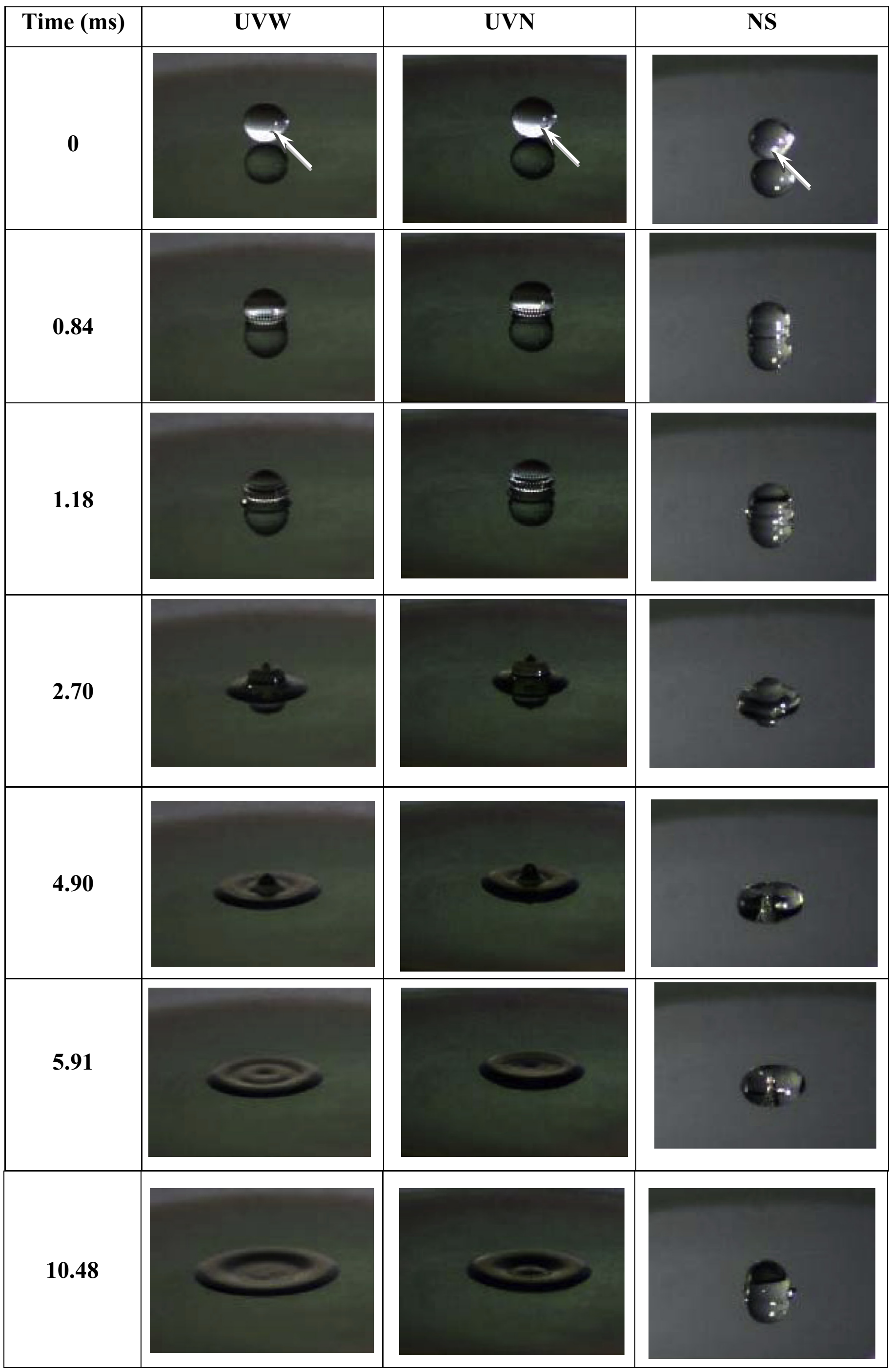

Fig. 5. The effect of static contact angle on the evaporation droplet dynamics on a solid surface at 60 °C (d_o = 2.4 mm).

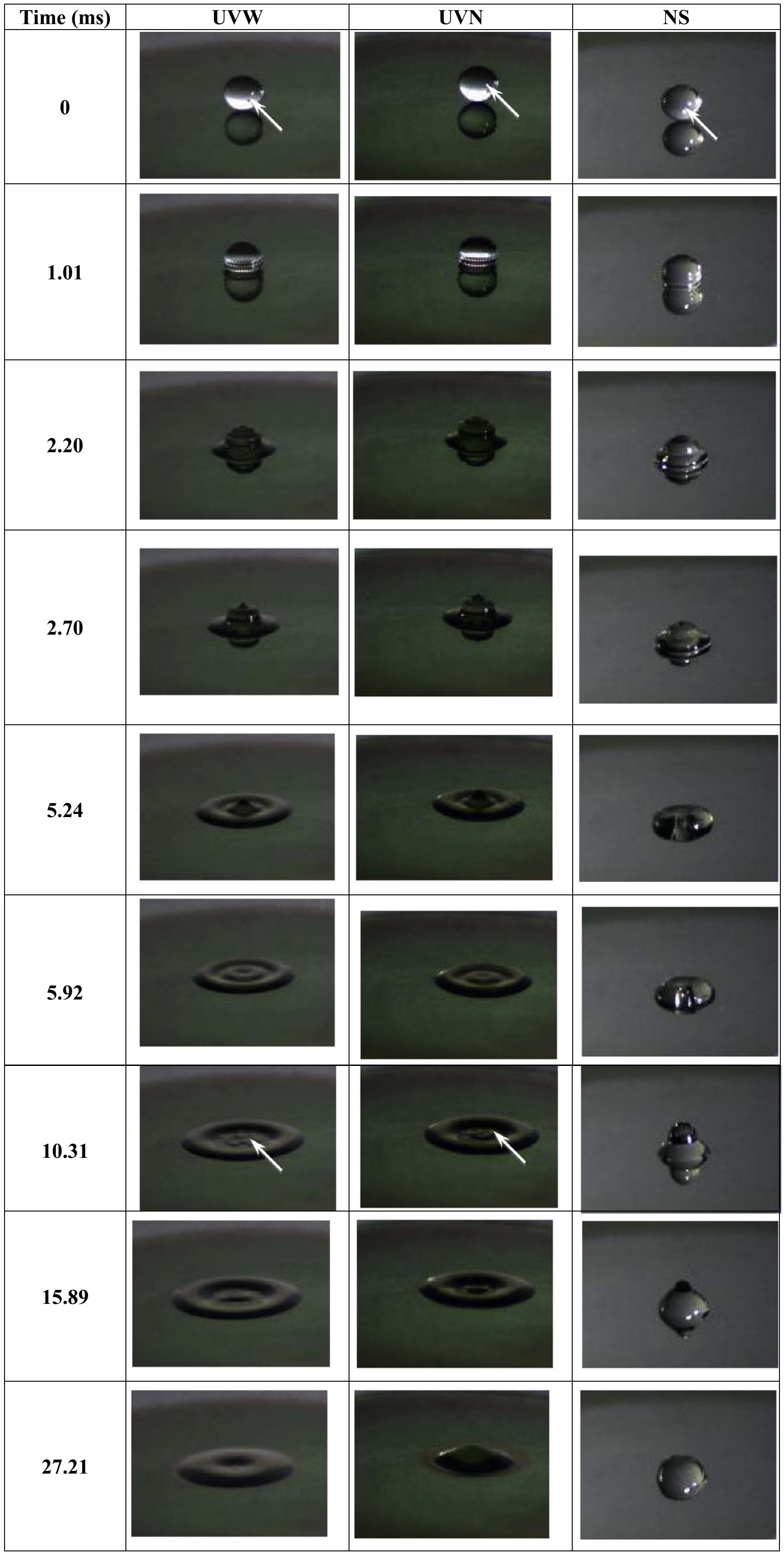

Fig. 6. The effect of static contact angle on the evaporation droplet dynamics on a solid surface at 100 °C (d_o = 2.4 mm).

2. Control of wettability

Heat transfer rate depends not only on the physical properties of the liquid, but also on the condition of the solid surface. The rate of heat removal from a heated component by a quenchant also depends on the ability of the liquid medium to wet and spread on its surface or its wettability [9]. A liquid is said to 'wet' a surface when the liquid spreads out spontaneously as a thin film across the said surface. This wettability can be characterized by the degree and the rate of wetting [10]. The degree of wetting is quantified by the contact angle formed at the three-phase interface.

Using force balance to describe the interaction of interfacial forces at this three phase interface, we obtain the Young–Dupre equation [11]:

$$\sigma_S = \sigma_{SL} + \sigma_L \cos\theta \quad (1)$$

where σ_S is the surface tension of solid, σ_L that of liquid, σ_{SL} the interfacial tension between solid and liquid and θ is the contact angle.

In the above equation, it can be clearly seen that the equilibrium of interfacial energies will determine the equilibrium contact angle (θ) formed at the three-phase contact point. For practical purposes, the liquid is said to wet the surface of solid when the contact angle is less than 90°. For contact angles greater than 90°, the liquid is considered as non-wetting. In non-wetting cases, the liquid drop spreads easily on the substrate surface and tends not to enter into pores or holes by capillary action.

It is expected that heat transfer and wetting characteristics of the quench medium are closely related. Improved wetting will enhance the rate of heat transfer from solid to liquid [12].

3. Wetting limit temperature

Hidaka et al. [13] remarked that the typical heat transfer characteristics of droplet evaporation is explained by using the relationship between the life time of droplet and the heated surface temperature in an evaporation curve as shown in Fig. 1. When

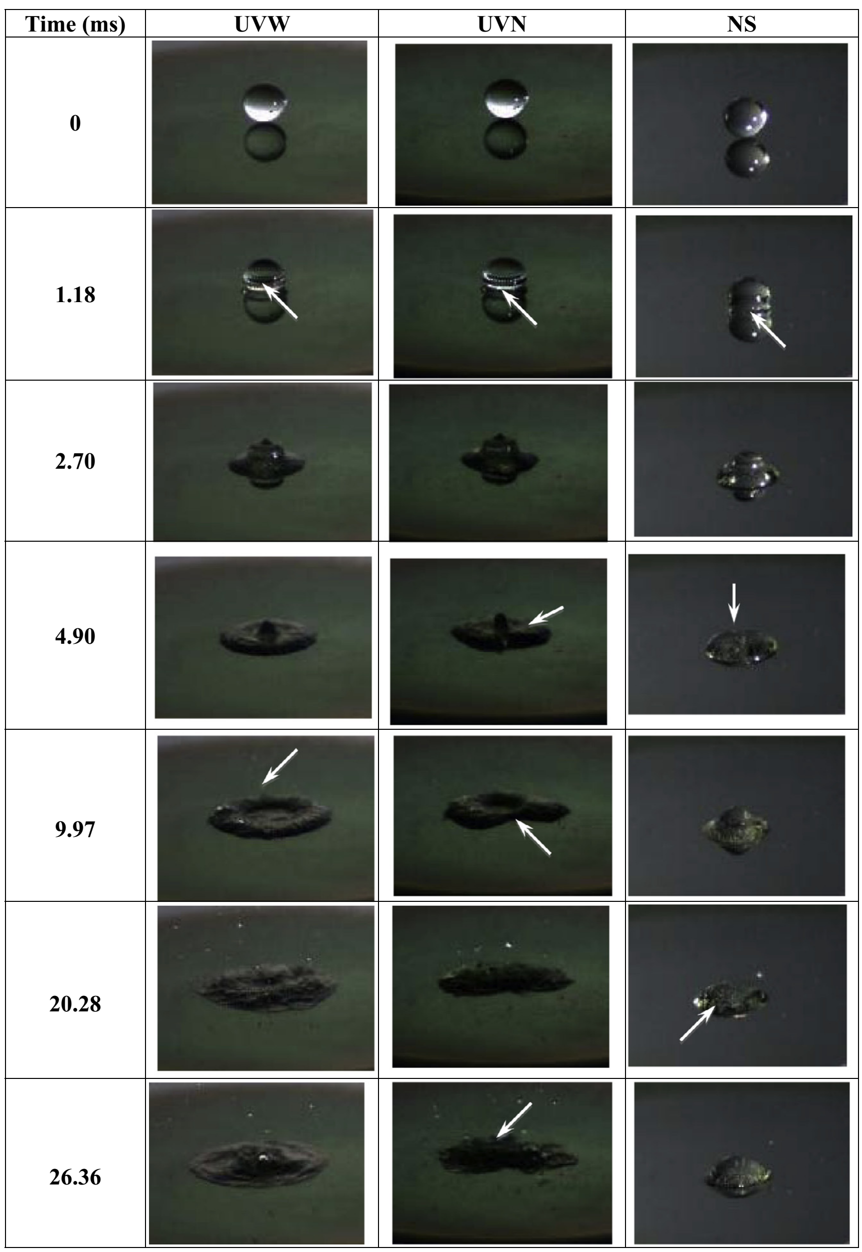

Fig. 7. The effect of static contact angle on the evaporation droplet dynamics on a solid surface at 180 °C (d_o = 2.4 mm).

the liquid droplet falls onto the hot surface, direct contact between liquid and solid occurs. If the surface temperature is moderate, the heat from the hot surface is first transferred to the liquid film by conduction and then evaporation occurs from the surface of the liquid film. As the surface temperature increases, evaporation time decreases to a minimum. The temperature at this point is the wetting limit temperature T_{WL}. As the surface temperature is further increased exceeding the wetting limit temperature, a vapor film is formed and the evaporation life time increases until a peak evaporation time. This point is the Leidenfrost point and the temperature at this point is defined as the Leidenfrost temperature T_{LP}. In the present experimental study, the wetting limit temperature

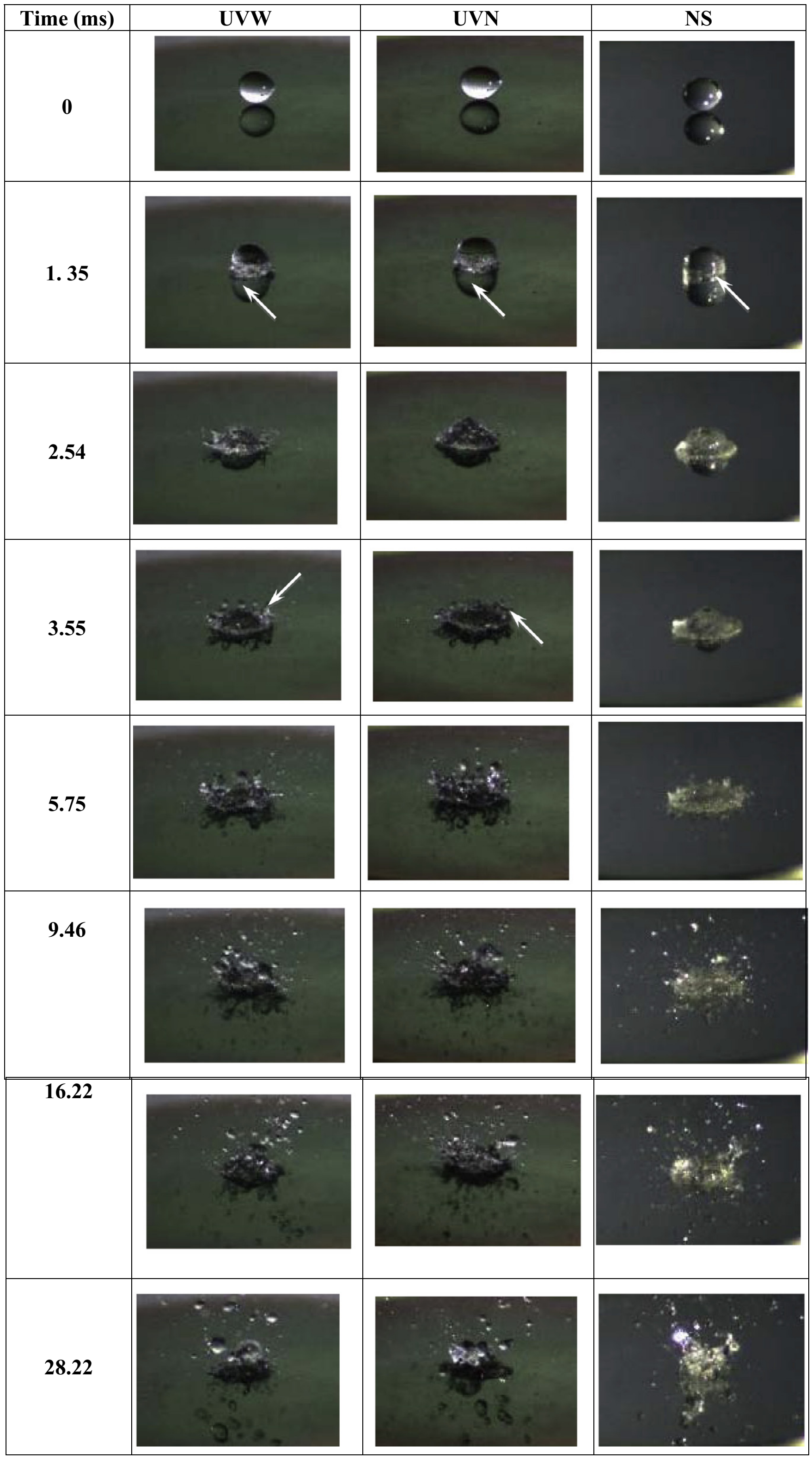

Fig. 8. The effect of static contact angle on the evaporation droplet dynamics on a solid surface at 250 °C (d_o = 2.4 mm).

T_{WL}, is taken as the characteristic temperature instead of the Leidenfrost temperature T_{LP}, because the heat transfer surface is too small to measure the Leidenfrost temperature accurately.

4. Experimental apparatus and procedures

The experimental setup used in the present study is shown in Fig. 2. The heating surface was adjusted with the heater wound in the lower part of the heat transfer block, in which the surrounding is insulated. The test surface temperature was measured by extrapolating the measurements of three thermocouples embedded in the heat transfer block at 10, 15, and 20 mm from the top surface. A water droplet was injected to the hot surface from the needle of an injection syringe. The distance between the heating surface and injection needle was fixed at 10 mm during the experiment. The micrometer was used to ensure the constant size of droplets. The droplet diameters were 1.90, 2.40 and 2.93 mm and the corresponding Weber numbers were 5.17, 5.67, and 6.72, respectively. The temperature of droplet was kept at 20 °C in all experimental runs.

Prior to each heat transfer experiment, this apparatus was also used to measure the static contact angle. For **UVW**, the static contact angle measurement was conducted to observe the change of contact angle during UV irradiation and after removal of UV irradiation. The details of the procedure of static contact angle measurement can be found in [14].

In the current study, the behavior of evaporating droplet was observed by using a high-speed video camera with a speed of 5908 fps and a shutter speed of 1/10,000 s. The most effective lighting for viewing the dynamic of droplets was found to produce the clear images when mounted opposite the camera at the same elevation. An image processing technique was developed to measure the droplet diameter as the function of time. The measurement was conducted by increasing the surface temperature from 58 °C to 340 °C. The temperature sensitivity device was 0.01 °C.

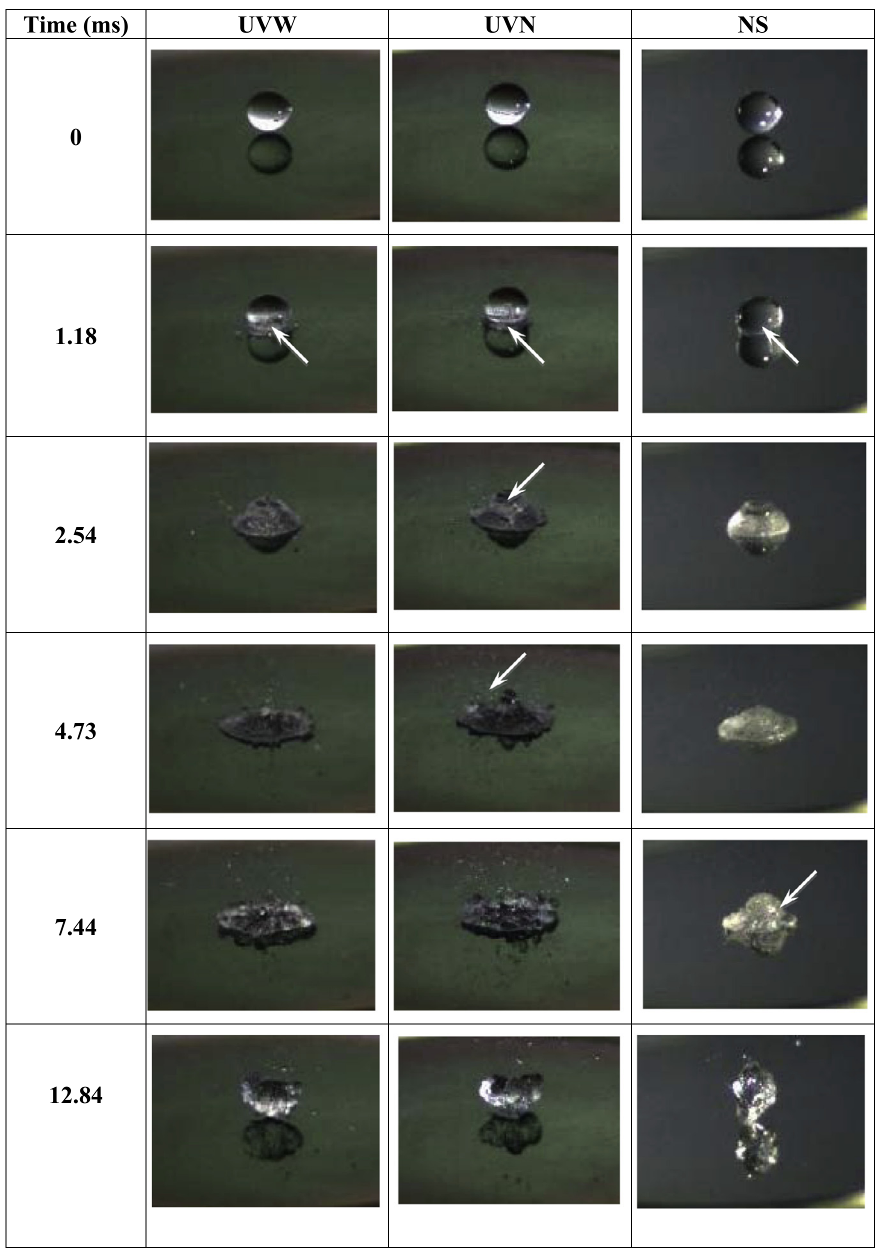

Fig. 9. The effect of static contact angle on the evaporation droplet dynamics on a solid surface at 340 °C (d_o = 2.4 mm).

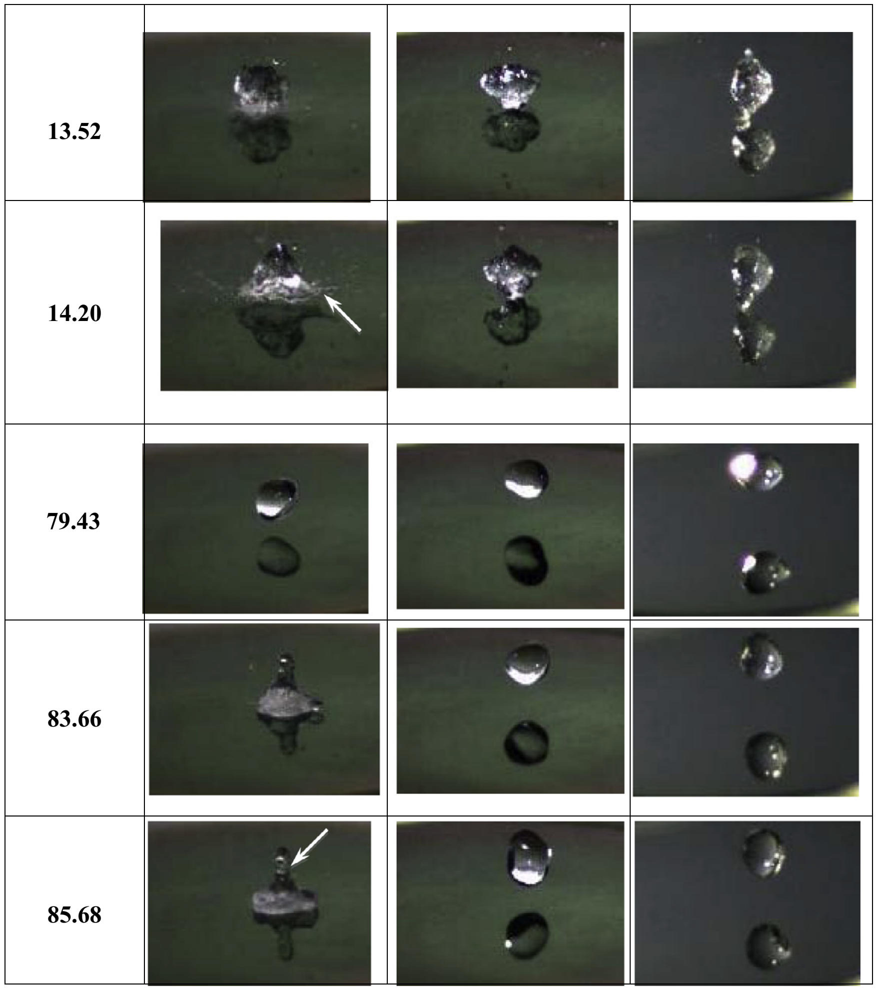

Fig. 9 (*continued*)

When the surface temperature is low and the evaporation time is relatively long, the droplet evaporation time was measured using timer. For short evaporation times, the evaporation time was obtained measured by using the frame count and relating it to the frame speed of the high-speed video camera.

In order to examine the effect of static contact angle as a single parameter, two modules of flat surfaces of stainless steel coated by TiO_2 were employed. The first module was irradiated by ultraviolet light to produce a hydrophilic surface, while the second one was not. The diameter of heat transfer surfaces was 30 mm, and the thickness of TiO_2 layer was 200 nm. The polished normal stainless steel without any TiO_2 coating was used as a comparison. Those are summarized in Table 1. Thus the experiment for the No. 3 was done only in the hydrophobic state.

To simplify the explanation in this paper, we use some abbreviations for the test surfaces by referring to their surface treatments. The abbreviations described in this paper are as follows; **UVW**: the stainless steel surface coated by TiO_2 and irradiated by ultraviolet, **UVN**: the stainless steel surface coated by TiO_2 without ultraviolet, and **NS**: polished stainless steel without any TiO_2 coating.

5. Results and discussions

Fig. 3 shows the results of static contact angle wettability tests of TiO_2 coated surfaces in which (a) and (b) correspond to the cases of the time variation of contact angle under ultraviolet irradiation and in dark conditions (without ultraviolet irradiation), respectively. Fig. 3(a) reveals that the contact angle decreases with the time under ultraviolet irradiation. The significant decrease was observed during first 25 min and then the contact angle decreases gradually. It reaches nearly 0° after 300 min. Next, how the contact angle recovers to hydrophobic state after shielded from ultraviolet is shown in Fig. 3(b). From this figure, it is revealed that the contact angle was around 10° after 300 min. The above results show that the TiO_2 coated surface hydrophobicity/hydrophilicity is easily manipulated by using UV irradiation.

Fig. 4 shows the evaporation curves for all the examined droplet diameters, in which (a)–(c) corresponds to the cases of the droplet diameters of 1.9 mm, 2.4 mm, and 2.9 mm, respectively. In the figures, the surface temperature is plotted against the evaporation time with the droplet diameter as a parameter. Since the droplet bounces out from the surface at higher surface temperature, the upper limit of measurement is the wetting limit temperature which is indicated in the figures as T_{WL}. As can be seen, T_{WL} varies with the surface treatments. Prior to each trial, the contact angle was measured at room temperature of which it was obtained that the initial contact angle for samples **NS**, **UVN** and **UVW** were 88°, 23° and 0°, respectively. The experimental results show that evaporation time decreases with the increase of the surface temperature and also decreases as initial contact angle decreases. It can be explained that the decrease of static contact angle increases the liquid film contact diameter, therefore the heat conduction through the liquid also increases. Consequently, the evaporation time will decrease. In addition, it was found that the evaporation time has a much higher dependency on contact angle and droplet diameter at low surface temperatures. This is shown by larger comparative differences of evaporation time as the evaporation time increases significantly in low surface temperature region. Meanwhile, at the higher surface temperature region the effect of droplet diameter is much is less significant.

Table 2 displays the effects of static contact angle and droplet diameter on the wetting limit temperature. As seen from the table, the wetting limit temperature increases with the decrease of contact angle. Comparison of droplet diameters for the same surface treatment shows that the droplet diameter plays an important role on the wetting limit temperature in such that the wetting limit temperature increases with the increase of the droplet diameter. Here, the larger the droplet diameter, the larger the mass of the droplet. Hence, the energy from the hot solid to boil the droplet also will increase. Therefore, the wetting limit temperature of the larger droplet diameter will be increased. Next, UV irradiation was found to increase the wetting limit temperature by about 10 K thus signifying that UV irradiation of TiO_2 coating is an effective technique to alter surface wettability as reported by [8] and that it can be used to enhance the phase change heat transfer.

Fig. 5 shows the deformation behavior of a water droplet impacting vertically on the surfaces with a surface temperature of 60°, thus exhibiting the droplet evaporation behavior below the boiling point. From the figure, it is observed that, a single bubble indicated by an arrow is seen in the center of the droplets at the impact point ($t = 0$ ms) which was caused by air entrapment. During the impact, a bubble can be created in the liquid if a cusp becomes enclosed. Similar phenomena were also reported by [15–17], who examined the collision dynamics of a water droplet on a hot solid surface. A sideway jetting of liquid due to the rapid pressure increase in the droplet during the impact was also clearly seen at $t = 2.70$ ms after the impact. An annular ridge of liquid film is formed due to surface tension gradients within the film resulting from temperature changes due to heat transfer from the hot surface. The ripple propagates ahead of the ridge. After the liquid films spread to their maximum diameter ($t = 4.9$ ms for **NS**), the droplet height increases slightly indicating the commencement of the constriction of the liquid film.

Comparison of the results for **NS**, **UVW** and **UVN** displayed in Fig. 5 reveals some differences. The structure of the liquid film was more spherical at **NS** compared to that of both **UVW** and **UVN**. It can be seen that the collision dynamics for **UVW** and **UVN** were similar. For both, at 2.70 ms after the impact, the droplet was observed to be flatten into a disc. However, as time progressed, the diameter of liquid film of **UVW** spread to a larger size than that of **UVN**. Relating this to the smaller static contact angle of **UVW**, it is possible to conclude that, below the water boiling point, the smaller the static contact angle, the larger the maximum diameter of liquid film after the impact.

The collision dynamics of the water droplets for a surface temperature of 100 °C is shown in Fig. 6. This characterizes the droplet evaporation behavior around the water boiling point at atmospheric pressure. The phenomena are quite similar with those at the surface temperature of 60 °C. Again we can see that at the impact point ($t = 0.0$ ms), a single bubble indicated by an arrow is observed in the center of droplet caused by the air entrapment. A number of circular and radial ridges as indicated by the arrows can be found at the center of the droplets both of **UVN** and **UVW** ($t = 10.31$ ms). The fact that the circular and radial ridges can be seen only on the surface with low contact angles (**UVN** and **UVW**), but not at **NS** implies that they were formed due the surface tension gradients created by temperature gradients within the droplets.

Fig. 7 depicts the collisions dynamics of water droplets for surface temperatures of 180 °C therefore within the transition regime

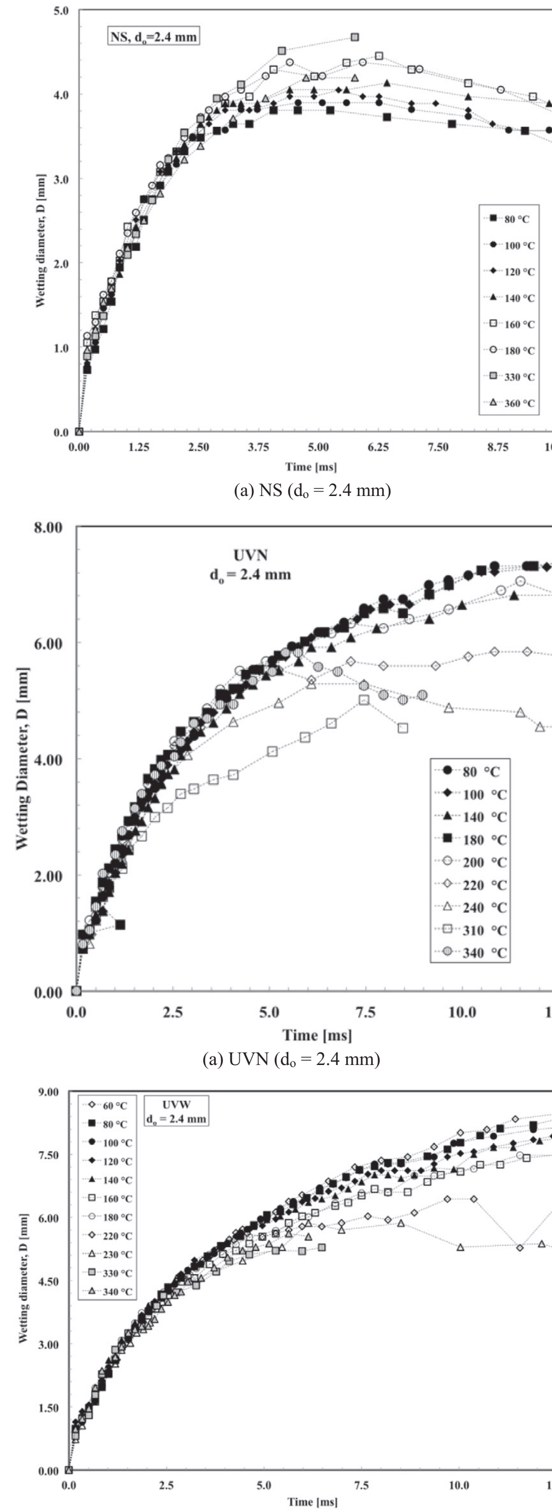

Fig. 10. The effect of surface temperature on the wetting diameter.

(below the wetting limit temperature as stated in Fig. 1). At the beginning time of the impact ($t < 2$ ms), the collision dynamics are quite similar with those at surface temperature of 100 °C. After this duration, the collision dynamics show a difference behavior. At $t = 4.90$ ms, a cluster of bubbles appeared in the ring of the droplet as indicated by the arrows in the figure. It is formed due to the nucleation on the liquid site rather than from the nucleation from the solid surfaces because the bubbles appear in the bulk of the liquid. At t = 9.97 mm, the bubble size is seen to increase due to the heat transfer from hot surface and the coalesence of the bubbles (c.f. **UVW**). Meanwhile, the droplet of **UVN** is significantly distorted, thereafter, the shape of droplet is unaxisymmetric. At

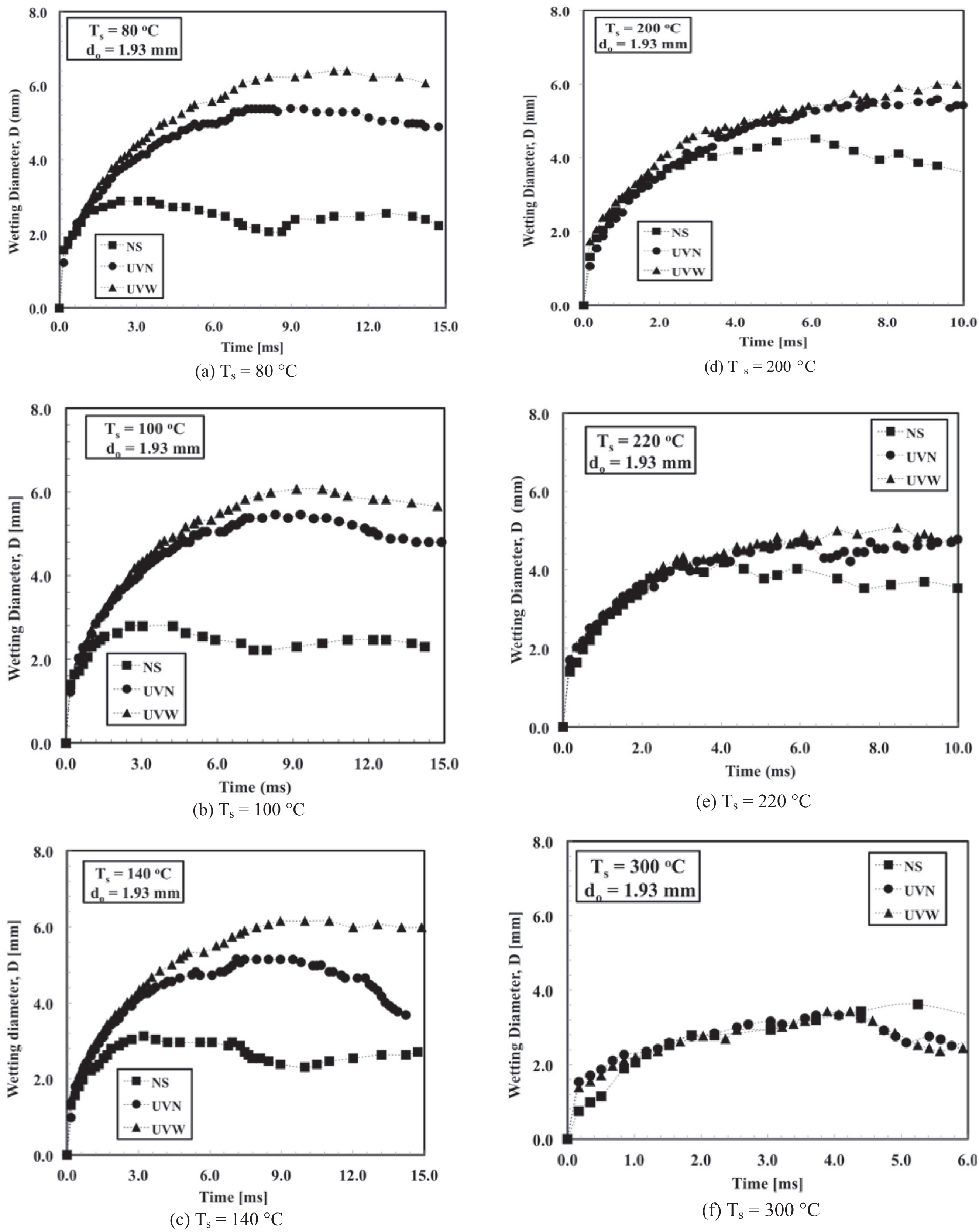

Fig. 11. The effect of surface treatment on the increment of the wetting diameter (d_o = 1.93 mm).

t = 20.28 ms, for all surface treatments, the droplets are filled with numerous bubbles on the circular periphery. The blowout of vapor bubbles in the form of secondary droplets can also be observed. It was noticed also that the static contact angle has a significant role on the collision dynamics on a hot solid surface in the boiling transition regime. At t = 26.36 ms, the wetting diameter of **UVW** appears as the largest diameter, followed by **UVN** and **NS**.

The collision dynamics for the surfaces at 250 °C are shown in Fig. 8. Here the droplet evaporation behavior near the wetting limit temperature was evaluated. Similar to previous observations, a

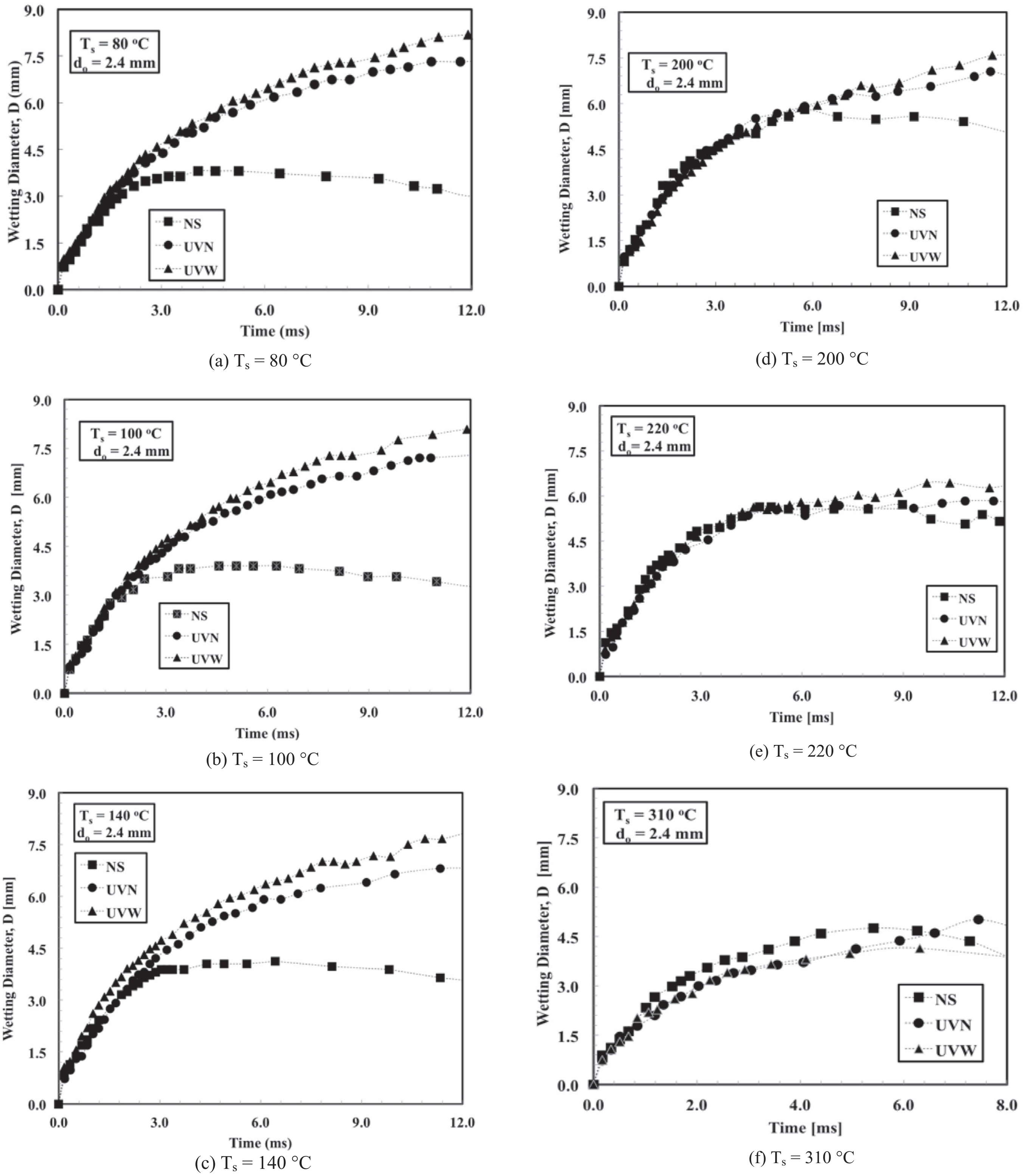

Fig. 12. The effect of surface treatment on the increment of the wetting diameter (d_o = 2.4 mm).

single bubble indicated by an arrow in the figure (at $t = 1.35$ ms in the figure) was observed in the center of droplet. However, contrarily to the observation made at a lower surface temperature, the bubbling occurs within the droplet by nucleate boiling of liquid contact with hot solid surface, and grows from the surface imperfection in which the liquid is trapped. Due to the surface temperature being much higher than the water boiling temperature, the liquid pressure is lower than its saturation pressure. Therefore, the cavitation takes part. Similar phenomena have been reported by [15]. This supports that the possible mechanism for the formation of the bubble at a temperature near the wetting limit temperature is cavitation within the liquid caused by a lowering of the liquid pressure to below its saturation vapor pressure.

Near the wetting limit temperature, it can be seen that the static contact angle does not play an important role on the droplet evaporation behavior. At around the wetting limit temperature, the modification of the surface treatments does not produce any considerable change in the morphology of bubble behaviors during

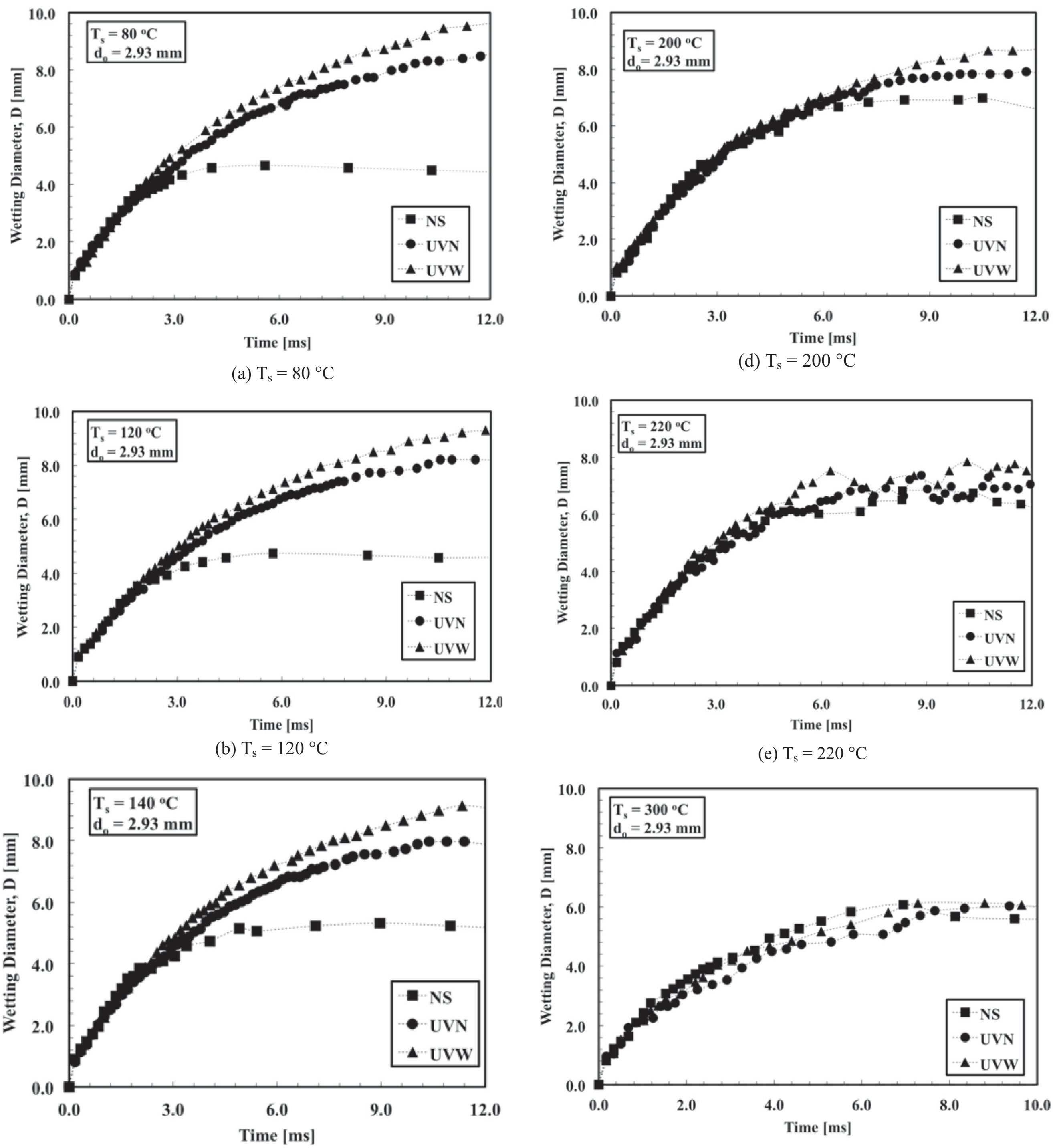

(a) T_s = 80 °C

(b) T_s = 120 °C

(c) T_s = 140 °C

(d) T_s = 200 °C

(e) T_s = 220 °C

(f) T_s = 300 °C

Fig. 13. The effect of surface treatment on the evolution of wetting diameter (d_o = 2.9 mm).

the evaporation on solid hot wall. In all cases, the droplet break-up appeared in the radial direction only after the formation of lamela crown (c.f. at t = 3.55 ms of **UVW** and **UVN**, and t = 5.75 ms of **NS**). It can be seen clearly from the images that many secondary droplets are jetted from all areas of the droplet and move upward to atmosphere, which contribute to secondary atomization. Formation of water jet prior to secondary atomization around the wetting limit temperature was also obtained by [7] for ethanol droplets impacting onto smooth surfaces. This means that effect of liquid surface tension is diminished.

Droplet evaporation and collision dynamics near the Leidenfrost temperature are depicted by Fig. 9. Here the surface temperature was set around 340 °C. The results reveal that above the Leidenfrost temperature, the collision dynamics and bubble behaviors during the droplet evaporation are similar for all the examined surface treatment/static contact angle. It is noted that the observed droplet morphologies include droplet impacts, spreads to maximum wetting diameter, recoils, and rebounds. A single bubble due to the cavitation is also observed in the center of droplet at the beginning of droplet impact. The blow out of vapor bubbles occurs at an earlier time (t = 2.54 ms of all the examined surface treatments) and many disintegrated droplets fly radially outward. After the maximum wetting diameter is reached, the droplet is elongated upward in the shape of bowling pin without any secondary droplet production (c.f. t = 83.66 ms of **UVW**) and rebounds off the hot solid surface as reported also by [17–19]. Considering the results for both 250 °C (Fig. 8) and 340 °C (Fig. 9), it can be seen that the static contact angle effects are diminished when the surface temperatures reaches the wetting limit temperature.

To investigate the influence of the surface temperature and static contact angle on the evolution of wetting diameter, the wetting diameter was measured by using image processing techniques. Fig. 10 shows the evolution of the wetting diameter as a function of the surface temperature. Fig. 10(a)–(c) correspond to the cases of **NS**, **UVN**, and **UVW**, respectively. Close observation from the figures reveals that in the lower transition regime, for first 2 ms after impact, the static contact angle does not affect the qualitative behavior of the wetting diameter. Here also, the wetting diameter seems to be independent of surface temperature. After this initial impact, the diameter increases to a maximum and afterwards gradually decreases with the time. The observed results are in agreement qualitatively with those of [15,18] who examined the wetting diameter during the droplet evaporation by using the difference surface treatments.

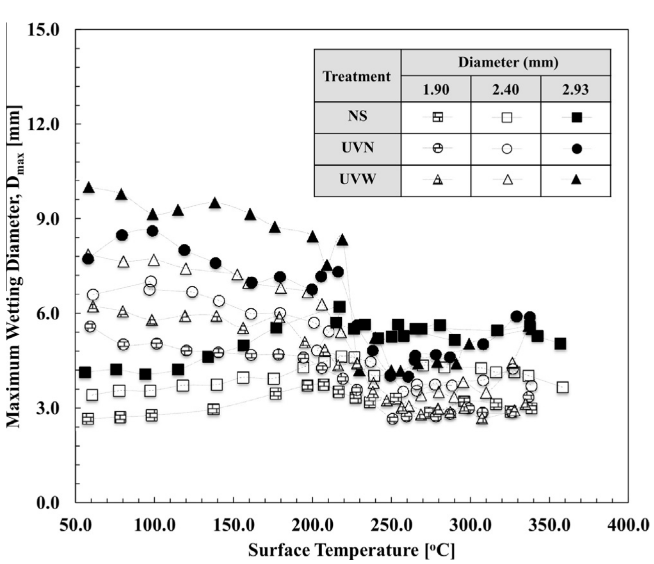

Fig. 14. The relationship between surface temperature and maximum wetting diameter.

Table 3
Different proposed empirical correlations to predict the maximum wetting diameter.

No	References (year)	Experimental correlation
1	Yang (1975) [22]	$\frac{We}{2} = \frac{3}{2}\beta_{\max}^2\left[1 + \frac{3We}{Re}\left(\beta_{\max}^2 \ln(\beta_{\max}) - \frac{\beta_{\max}^2 - 1}{2}\right)\left(\frac{\mu_{drop}}{\mu_{wall}}\right)^{0.14}\right] - 6$ (Kurabayashi and Yang equation)
2	Akao et al. (1980) [23]	$\frac{R_{\max}}{R_o} = 0.613We^{0.39}$
3	Chandra and Avedisian (1991) [15]	$\frac{3We}{2Re}\beta_{\max}^4 + (1 - \cos\theta)\beta_{\max}^2 - \left(\frac{We}{3} + 4\right) = 0$
4	Senda et al. (1997) [24]	$\frac{D_{\max}}{D_o} = 1.0 + 0.463We^{0.345}$
5	Healy et al. (2001) [21]	$\beta_{\max,corr} = \beta_{\max,KY}\left(\frac{45}{\theta}\right)^{0.241}$
6	Roisman (2009) [25]	$\frac{D_{\max}}{D_o} = 0.87Re^{1/5} - 0.40Re^{2/5}We^{-1/2}$

Figs. 11–13 show the effects of the static contact angle on the wetting diameter during the droplet evaporation on a hot solid surface, in which Figs. 11–13 corresponds to the cases of droplet diameter of 1.93 mm, 2.4 mm, and 2.9 mm, respectively. From the figures, it can be seen that the static contact angle has a significant effect on the wetting diameter during the droplet evaporation on a hot solid surface below the wetting limit temperatures of correspond static contact angle. Thus, the higher the static angle, the lower the wetting diameter. At the early stages after impact, the evolution of wetting diameter is independent relatively of static contact angle. When the surface temperature is increased, the effect of ultraviolet radiation is apparent only at a later time after the initial impact. The above are observed for all droplet diameters.

The maximum wetting diameter is an important aspect that is of interest in the heat transfer studies [20]. Fig. 14 displays the relation between droplet maximum wetting diameter and surface temperature for all observed droplet diameters and surface treatments. Close observation of the figure revealed that the maximum wetting diameter is relatively independent of when the surface temperature is higher than 250 °C (around the wetting limit temperature) as has already discussed above. Below 250 °C, the maximum wetting diameter increases with increased static contact angle and droplet diameter. Here it is apparent that the static contact angle has an important role on the maximum and evolution of droplet wetting diameters below the wetting limit temperature, and are the important results from the present work, whereas it has never reported in the open literature before.

Presently several empirical correlations [15,21–25] have been devised to calculate the maximum wetting diameter during the evaporation droplet on a hot solid surface, and they are tabulated in Table 3. The empirical correlations include the Weber number, Reynolds number, fluid viscosity, and liquid contact angle. It should be noted that user adjustment in the developed empirical correlations still cannot be avoided. For example, Healey et al. [21] incorporated the liquid contact angle as a correction factor (denominator) in the original Kurabayashi and Yang correlation. In regards to the current work, if we implement the contact angle of the UVW case in the present experimental data, whereas θ is equal to 0°, the correction factor would be equal to infinity. Hence the maximum wetting diameter could not be predicted. Therefore, the effect of contact angle expressed by Healy et al.'s correlations will not correctly predict the data presented in this work. Thus, the future work is needed to develop an improved empirical correlation and numerical solution on the basis of the physics involved in determining the maximum wetting diameter.

6. Concluding remarks

An experimental study on the effects on static contact angle on the evaporation droplet on hot solid surface has been carried-out. The static contact angles of stainless steel surfaces were modified by using the TiO_2 coating and ultraviolet irradiation. Their effects on the main parameters, such as wetting limit temperature, interfacial behavior of the droplet, evolution and maximum wetting diameter, were studied. The results are summarized as follows:

1. The static contact angle plays an important role on the wetting limit temperature during the single droplet evaporation on a hot wall. The higher the static contact angle, the lower the wetting limit temperature.
2. Below the wetting limit temperatures it is found that the surface temperature, the droplet diameter, and static contact effect the evolution of wetting diameter of single droplet during the single droplet evaporation on a hot wall. That is the higher the droplet diameter, the higher the wetting diameter. Next, the maximum wetting diameter increases with the decrease of static contact angle.
3. The ultraviolet irradiation on the TiO_2 surface does not change the qualitative behavior of the evolution of wetting diameters during the droplet evaporation on a hot solid.
4. From the review of the available experimental correlations regarding the maximum wetting diameter during the single droplet evaporation on a hot wall, it is found that the static contact angle was not considered as an important parameter, therefore, a future work on the development of new experimental correlation and numerical model on this topic is needed.

References

[1] J.D. Bernardin, C.J. Stebbins, I. Mudawar, Mapping of impact and heat transfer regimes of water drops impinging on a polished surface, Int. J. Heat Mass Transfer 40 (2) (1997) 247–267.
[2] I. Mudawar, W.S. Valentine, Determination of the local quench curve for spray cooled metallic surfaces, ASM J. Heat Treat. 7 (1989) 107–121.
[3] W.P. Klinzing, J.P. Rozzi, I. Mudawar, Film and transition boiling correlations for quenching of hot surfaces with water sprays, ASM J. Heat Treat. 9 (1992) 91–103.
[4] J.D. Bernardin, I. Mudawar, Film boiling heat transfer of droplet streams and sprays, Int. J. Heat Mass Transfer 40 (11) (1997) 2579–2593.
[5] Y.M. Qiao, S. Chandra, Spray cooling enhancements by addition of a surfactant, ASME J. Heat Transfer 120 (1998) 92–98.
[6] S.L. Manzello, J.C. Yang, On the collision dynamics of a water droplet containing an additive on a heated solid surface, Proc. R. Soc. London A 458 (2002) 2417–2444.
[7] A.S. Moita, A.I.N. Moreira, Drop impacts onto cold and heated rigid surfaces: morphological comparisons, disintegration limits and secondary atomization, Int. J. Heat Fluid Flow 28 (4) (2007) 735–752.
[8] M. Miyauchi, N. Kieda, S. Hishita, T. Mitsuhashi, A. Nakajima, T. Watanabe, K. Hashimoto, Reversible wettability control of TiO_2 surface by light irradiation, Surf. Sci. 511 (1–3) (2002) 401–407.
[9] S.J. Gokhale, J.L. Plawsky, P.C. Wayner, Experimental investigation of contact angle, curvature, and contact line motion in dropwise condensation and evaporation, J. Colloid Interface Sci. 259 (2) (2003) 354–366.
[10] S. Sikalo, C. Tropea, E.N. Ganic, Dynamic wetting angle of a spreading droplet, Exp. Therm. Fluid Sci. 29 (7) (2005) 795–802.
[11] J.D. Bernardin, I. Mudawar, C. Walsh, E. Franses, Contact angle temperature dependence for water droplets on practical aluminum surfaces, Int. J. Heat Mass Transfer 40 (5) (1997) 1017–1033.
[12] P. Fernandes, K.N. Prabhu, Comparative study of heat transfer and wetting characteristics of conventional and bioquenchants, Int. J. Heat Mass Transfer 51 (3–4) (2008) 526–538.
[13] S. Hidaka, A. Yamashita, Y. Takata, Effect of contact angle on wetting limit temperature, Heat Transfer Asian Res. 35 (7) (2006) 513–526.
[14] Y. Takata, S. Hidaka, A. Yamashita, H. Yamamoto, Evaporation of water drop on plasma-irradiated hydrophylic surface, Int. J. Heat Fluid Flow 25 (2) (2004) 320–328.
[15] S. Chandra, C.T. Avedisian, On the collision of a droplet with a solid surface, Proc. R. Soc. London A 432 (1991) 13–41.
[16] H. Fujimoto, H. Shiraishi, N. Hatta, Evolution of liquid/solid contact area of a drop impinging on a solid surface, Int. J. Heat Mass Transfer 43 (9) (2000) 1673–1677.
[17] H. Fujimoto, Y. Oku, T. Ogihara, H. Takuda, Hydrodynamics and boiling phenomena of water droplets impinging on hot solid, Int. J. Multiphase Flow 36 (8) (2010) 620–642.
[18] S.L. Manzello, J.C. Yang, An experimental investigation of water droplet impingement on a heated wax surface, Int. J. Heat Mass Transfer 47 (8–9) (2004) 1701–1709.
[19] C.K. Huang, V.P. Carey, The effects of dissolved salt on the Leidenfrost transition, Int. J. Heat Mass Transfer 50 (1–2) (2007) 269–282.
[20] S.G. Kandlikar, M.E. Steinke, Contact angles of droplets during spread and recoil after impinging on a heated surface, Trans IChemE 79 (2001) 491–498.
[21] W.M. Healy, J.G. Hartley, S.I. Abdel-Khalik, Surface wetting effects on the spreading of liquid droplets impacting a solid surface at low Weber numbers, Int. J. Heat Mass Transfer 44 (1) (2001) 235–240.
[22] W.J. Yang, Theory on vaporization and combustion of liquid drops of pure substances and binary mixtures on heated surfaces, Technical Report 535, Institute of Space and Aeronautical Science, University of Tokyo, Tokyo, 1975.
[23] A. Akao, K. Araki, S. Mori, A. Moriyama, Deformation behaviors of a liquid droplet impinging on to hot metal surface, Trans. Iron Steel Inst. Jpn. 20 (1980) 737–743.
[24] J. Senda, T. Kanda, M. Al-Roub, P.V. Farrell, T. Fukami, H. Fujimoto, Modeling spray impingement considering fuel film on the wall, SAE Paper 970047, 1997, pp. 37–51.
[25] V.I. Roisman, Inertia dominated drop collisions. II. An analytical solution of the Navier–Stokes equations for a spreading viscous film, Phys. Fluids 21 (2009) 052104.